Author(s): Wallén, Henrik & Kettunen, Henrik & Sihvola, Ari

Title: Anomalous absorption, plasmonic resonances, and invisibility of radially anisotropic spheres

Year: 2015

Version: Final published version

Please cite the original version:

Wallén, Henrik & Kettunen, Henrik & Sihvola, Ari. 2015. Anomalous absorption, plasmonic resonances, and invisibility of radially anisotropic spheres. Radio Science. Volume 50, Issue 1. 18-28. 0048-6604 (printed). DOI: 10.1002/2014RS005534.

AGU PUBLICATIONS

Radio Science

RESEARCH ARTICLE

10.1002/2014RS005534

Special Section:
2013 Hiroshima International Symposium on Electromagnetic Theory

Anomalous absorption, plasmonic resonances, and invisibility of radially anisotropic spheres

Henrik Wallén[1], Henrik Kettunen[2], and Ari Sihvola[1]

[1]Department of Radio Science and Engineering, Aalto University School of Electrical Engineering, Espoo, Finland, [2]Department of Mathematics and Statistics, University of Helsinki, Helsinki, Finland

Key Points:
- A sphere with hyperbolic radial anisotropy can exhibit anomalous absorption
- The quasistatic results are verified by puncturing the origin and adding losses
- Good agreement between Mie series and quasistatics is found

Correspondence to:
H. Wallén,
henrik.wallen@aalto.fi

Citation:
Wallén, H., H. Kettunen, and A. Sihvola (2015), Anomalous absorption, plasmonic resonances, and invisibility of radially anisotropic spheres, *Radio Sci.*, *50*, 18–28, doi:10.1002/2014RS005534.

Received 28 MAY 2014
Accepted 11 DEC 2014
Accepted article online 13 DEC 2014
Published online 13 JAN 2015

Abstract This article analyzes the response of a sphere with radially anisotropic permittivity dyadic (RA sphere), in both the electrostatic and full electrodynamic settings. Depending on the values and signs of the permittivity components, the quasistatic polarizability of the RA sphere exhibits several very different interesting properties, including invisibility, field concentration, resonant singularities, and emergent losses. Special attention is given to the anomalous losses that appear in the case of certain hyperbolic anisotropy values. We show that their validity can be justified in a limiting sense by puncturing the sphere at the origin and adding a small imaginary part into the permittivity components. A hyperbolic RA sphere with very small intrinsic losses can thus have significant effective losses making it an effective absorber. With different choices of permittivities, the RA sphere could also perform as a cloak or a sensor. The Mie scattering results by an RA sphere are used to justify the quasistatic calculations. It is shown that in the small parameter limit the absorption efficiency of an RA sphere is nonzero for certain lossless hyperbolic anisotropies. The absorption and scattering efficiencies agree with the quasistatic calculations fairly well for spheres with size parameters up to 1/3.

1. Introduction

The electrostatic problem involving a radially anisotropic (RA) sphere has been considered in several publications in the past. Originally, *Schulgasser* [1983] considered the bounds of the effective (heat) conductivity of an assemblage of spherical radially anisotropic crystals. Hence, the RA sphere has also been referred to as a *Schulgasser* sphere. This study was continued by *Helsing and Helte* [1991] who derived a model for the effective (electric) conductivity for the *Schulgasser assemblage*. Layered RA spheres, and even RA spheroids, were considered as models for a human head for electroencephalography purposes by *de Munck* [1988]. The image solutions for an RA sphere with an external and internal point source were derived by *Sten* [1995]. He was also probably the first who introduced the expression *RA sphere*. Recently, *Rimpiläinen et al.* [2012] derived the solution for the Laplace equation in a more general case of a *systropic* sphere whose three permittivity components, given in spherical coordinates, are all allowed to be unequal.

Probably, the first occurrence of an RA material in the literature is, however, *Roth and Dignam* [1973], where light scattering is studied from a spherical particle that is coated by a radially anisotropic layer. On the other hand, the first numerical results based on full Mie scattering theory were presented much later by *Wong and Chen* [1992]. Since then, scattering from layered RA spheres has been studied, e.g., by *Kiselev et al.* [2002] using a *T* matrix method. Mie scattering coefficients for an RA sphere with both electric and magnetic anisotropy were derived by *Qiu et al.* [2007].

Mie scattering from other kinds of anisotropic spheres can also be found in the literature: for instance ordinary uniaxial [*Geng et al.*, 2004] and plasma anisotropic [*Geng et al.*, 2003] spheres, with the anisotropy defined in Cartesian coordinates. Earlier *Monzon* [1989] also considered scattering from a sphere with a general rotationally symmetric anisotropy defined in spherical coordinates. See also the fairly extensive review in *Qiu et al.* [2010] for more references.

Radially anisotropic geometries are present, for example, in liquid crystal physics. Liquid crystal materials consist of *nematic* microdroplets dispersed into a polymer matrix. With a certain orientational director configuration these droplets resemble RA spheres. Light scattering from small nematic droplets has been studied by approximative methods by *Žumer and Doane* [1986], *Žumer* [1988], and *Karacali et al.* [1997].

More recently, RA spheres have appeared in metamaterials research, where the material parameters can also be assumed negative. Scattering from a plasmonic RA sphere was considered, e.g., by *Qiu et al.* [2010]. Quasistatic cloaking using spherical RA coatings has also been considered in several papers. *Gao et al.* [2008] studied the cancelation of the dipole moments of both electrically and magnetically radially anisotropic spheres using suitable RA coatings. *Qiu et al.* [2009] further analyzed a more complicated case using inhomogeneous RA coatings. *Kettunen et al.* [2013], instead, considered using only positive permittivity components with extreme anisotropy, which would create an invisible Faraday cage that could hide any objects small enough independent of their shape or material. This cloaking approach is also illustrated in section 2.3 in this paper.

In metamaterials research, media with extremely strong anisotropies have attracted attention. In particular, if some of the eigenvalues (principal components) of the permittivity or permeability dyadics of the medium are of opposite signs, the wave dispersion characteristics may be very intricate. Such media have been called *indefinite* metamaterials [*Smith and Schurig*, 2003]. Recently, the term *hyperbolic* anisotropy has become more commonly used for such material tensors [*Noginov et al.*, 2013]. The recent article by *Poddubny et al.* [2013] gives an extensive review on applications and realizations of hyperbolic metamaterials.

The considered hyperbolic metamaterials are usually based on Cartesian geometries. Here instead, we discuss a hyperbolic nonmagnetic RA sphere, whose permittivity is anisotropic with respect to the spherical coordinates (r, θ, φ). A peculiarity of a lossless hyperbolic RA sphere is that it shows anomalous lossy response in both static and dynamic cases. This anomalous enhancement of absorption, or nondissipative damping, is also discussed in *Qiu and Luk'yanchuk* [2008]. The physics of similar anomalous absorption (or gain) given rise by the sharp corners of a structure consisting of two conjoined hemicylinders is discussed in depth by *Mohammadi Estakhri and Alù* [2013].

In this paper we continue the work with a thorough treatment of the RA sphere in both the static and dynamic case. In particular, we analyze the small size limiting behavior of the full-wave electromagnetic scattering problem. To be more specific, we consider an RA sphere of radius a and permittivity

$$\bar{\bar{\varepsilon}} = \varepsilon_0 \left[\varepsilon_{\mathrm{r}} \mathbf{u}_r \mathbf{u}_r + \varepsilon_{\mathrm{t}} \left(\mathbf{u}_\theta \mathbf{u}_\theta + \mathbf{u}_\varphi \mathbf{u}_\varphi\right)\right] \tag{1}$$

centered at the origin of the spherical coordinate system (r, θ, φ). The excitation is either a uniform static electric field or a linearly polarized plane wave.

Relative permittivity less than one is not physically reasonable at zero frequency, but even negative permittivity with relatively small losses can be found at high enough frequencies [*Johnson and Christy*, 1972]. Our quasistatic treatment must, therefore, be understood as an approximation where the sphere is small enough compared with the wavelength. In both the quasistatic and full dynamic case, we can assume that we operate on a fixed frequency, while the radius a is adjusted as needed. In this paper, we assume an idealized RA sphere, with small or vanishing material losses and leave more detailed realization ideas for future work.

In section 2, we derive the conditions for anomalous absorption, plasmonic resonances, and invisibility in the static case and study the effect of small losses and the removal of the origin of the sphere. A dynamic treatment of the scattering and absorption by an RA sphere is performed in section 3 where we find a good agreement between the static and dynamic solutions. The main results are summarized in section 4. This paper is an extended version of the conference presentation *Wallén et al.* [2013].

2. Electrostatic Solution

The electrostatic potential in an anisotropic sourceless medium satisfies the (generalized) Laplace equation

$$\nabla \cdot \left(\bar{\bar{\varepsilon}} \cdot \nabla \phi\right) = 0, \tag{2}$$

whose solution can be found using separation of variables when the anisotropy fits into one of the usual coordinate systems. In the RA case (1), the general solution can be written as $\phi(r, \theta, \varphi) = R(r)T(\theta)P(\varphi)$, where the component functions are

$$R(r) = A\, r^{\nu} + B\, r^{-\nu-1}, \tag{3}$$

$$T(\theta) = C\,\mathrm{P}_n^m(\cos\theta) + D\,\mathrm{Q}_n^m(\cos\theta), \tag{4}$$

$$P(\varphi) = E\cos(m\varphi) + F\sin(m\varphi), \tag{5}$$

where P_n^m and Q_n^m are the associated Legendre functions and the parameter ν is

$$\nu = \nu(n) = -\frac{1}{2} + \sqrt{n(n+1)\frac{\varepsilon_\mathrm{t}}{\varepsilon_\mathrm{r}} + \frac{1}{4}}. \tag{6}$$

The constants $A, \ldots, F$ are determined by the boundary and interface conditions, and a double infinite sum over $n = 0, 1, \ldots$ and $m = 0, 1, \ldots, n$ is needed in the most general case. The derivation of this general solution (3)–(6) is a trivial extension of the rotationally symmetric special case $m = 0$, whose solution is well described by *Helsing and Helte* [1991] and also *Sten* [1995].

The radial anisotropy can be interpreted as a stretching in the radial direction, while the angular part $T(\theta)P(\varphi)$ is exactly the same as for an isotropic medium. In the isotropic case ($\varepsilon_\mathrm{r} = \varepsilon_\mathrm{t}$), we simply get $\nu = n$.

2.1. Intact RA Sphere

Let us first derive the electrostatic solution for an intact RA sphere assuming positive permittivity and thereafter discuss the validity of the solution for negative and especially hyperbolic permittivity.

Assume that the RA sphere of radius a is placed in an external uniform field that is oriented along the z axis. The external potential can then be expressed as

$$\phi_0(r,\theta) = -U_0\frac{r}{a}\cos\theta = -U_0\frac{r}{a}\mathrm{P}_1^0(\cos\theta), \tag{7}$$

and we seek a solution in the form

$$\phi(r,\theta) = \begin{cases} \phi_\mathrm{i}(r,\theta), & r < a, \\ \phi_0(r,\theta) + \phi_\mathrm{s}(r,\theta), & r > a, \end{cases} \tag{8}$$

where the internal and scattered potentials are

$$\phi_\mathrm{i}(r,\theta) = A\left(\frac{r}{a}\right)^\nu \cos\theta, \quad \nu = \nu(1), \tag{9}$$

$$\phi_\mathrm{s}(r,\theta) = B\left(\frac{r}{a}\right)^{-2}\cos\theta. \tag{10}$$

The solution can only contain the same angular functions as the excitation, since the angular functions (or spherical harmonics) are orthogonal over the full solid angle. The radial functions are chosen so that ϕ_s vanishes as $r \to \infty$ and ϕ_i is finite at the origin. (Notice that $\nu > 0$ when $\varepsilon_\mathrm{t}/\varepsilon_\mathrm{r} > 0$.) The normalization r/a is introduced for convenience.

Enforcing the interface conditions

$$\phi_\mathrm{i} = \phi_0 + \phi_\mathrm{s}, \quad \varepsilon_\mathrm{r}\frac{\partial\phi_\mathrm{i}}{\partial r} = \frac{\partial\phi_0}{\partial r} + \frac{\partial\phi_\mathrm{s}}{\partial r} \tag{11}$$

on the surface $r = a$ of the RA sphere gives the constants

$$A = \frac{-3U_0}{\varepsilon_\mathrm{r}\nu + 2}, \quad B = \frac{(\varepsilon_\mathrm{r}\nu - 1)U_0}{\varepsilon_\mathrm{r}\nu + 2}. \tag{12}$$

The scattered potential ϕ_s is the same as the potential of a z directed point dipole with the dipole moment $p = 4\pi a^2\varepsilon_0 B$ at the origin in free space. The ratio between this induced dipole moment and the external field is conveniently described by the *normalized polarizability*

$$\alpha = \frac{p}{\varepsilon_0 E_0 V} = \frac{3B}{U_0}, \tag{13}$$

where $E_0 = U_0/a$ and V is the volume of the sphere. The normalized polarizability of the RA sphere can thus be written in the form

$$\alpha = 3\frac{\varepsilon_\mathrm{eff} - 1}{\varepsilon_\mathrm{eff} + 2}, \tag{14}$$

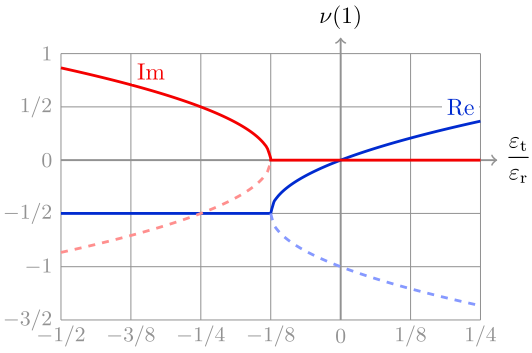

Figure 1. The exponent $\nu(1)$ as function of $\varepsilon_t/\varepsilon_r$. The dashed line is the other solution $-\nu(1)-1$.

if we define the effective permittivity

$$\varepsilon_{\text{eff}} = \varepsilon_r \nu(1) = \frac{\varepsilon_r}{2}\left(-1+\sqrt{1+8\varepsilon_t/\varepsilon_r}\right). \quad (15)$$

Since (14) is exactly the same as the normalized polarizability of a homogeneous sphere with relative permittivity ε_{eff}, this solution can also be interpreted as an *internal homogenization*, using the terminology of *Chettiar and Engheta* [2012].

This electrostatic solution is mathematically correct and physically valid if both permittivity components ε_r and ε_t are real and positive. The solution also seems reasonable if both ε_r and ε_t are real and negative, except perhaps for the special case when $\varepsilon_{\text{eff}} = -2$, where the infinite polarizability should be interpreted carefully, as pointed out by *Mei et al.* [2013].

The solution is, however, quite puzzling when the anisotropy is indefinite or hyperbolic, that is, when ε_r and ε_t are real with opposite signs. In that case, the exponent $\nu = \nu(1)$ is negative or complex with a negative real part, as shown in Figure 1, and consequently, the potential is singular at the origin. In the hyperbolic case, the choice of the radial solution; i.e., the exponent ν or $-\nu-1$ is not immediately obvious. Choosing the negative branch of the square root in (6) is tantamount to choosing $-\nu(1)-1$ instead of $\nu(1)$. To avoid too singular behavior of the potential, we should obviously always make the choice which leads to a positive or less negative exponent. For $\varepsilon_t/\varepsilon_r > -1/8$ this means that we should choose ν. When $\varepsilon_t/\varepsilon_r < -1/8$, both exponents have a negative real part which means that the electrostatic potential is singular at the origin independently of the choice. In that case, the two exponents ν and $-\nu-1$ are complex conjugates of each other, which leads to complex conjugate pairs of ε_{eff}, and we should clearly choose the passive (lossy) solution rather than the active one.

A more thorough analysis in sections 2.4 and 2.5 shows that this quasistatic solution is, after all, physically sound in a certain low-loss limiting sense. Let us, however, first simply assume that the quasistatic normalized polarizability given by (14) and (15) is valid for any real ε_r and ε_t and study the interesting behavior of α in the two-dimensional $\varepsilon_r\varepsilon_t$ plane.

2.2. Anomalous Absorption

The above-derived quasistatic polarizability is complex when $\varepsilon_t/\varepsilon_r < -1/8$, corresponding to two regions in the $\varepsilon_r\varepsilon_t$ plane in Figure 2. A complex α means that the sphere is effectively lossy. This is counterintuitive since the material parameters ε_r and ε_t are real, and hence, we could call this phenomenon *anomalous absorption*.

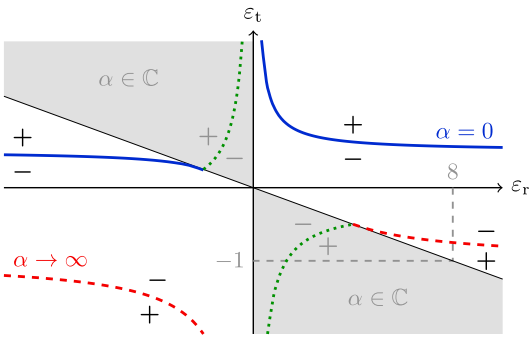

Figure 2. The polarizability of the intact RA sphere is well defined in the first and third quadrants of the $\varepsilon_r\varepsilon_t$ plane, but the potential is singular at the origin if $\varepsilon_t/\varepsilon_r < 0$. In the shaded region both the potential and the polarizability appear to be complex. The locations where the polarizability vanishes (solid line) and is singular (dashed line) are also plotted. The real part of the polarizability is zero in the complex region at the dotted line. The plus and minus signs are the signs of (the real part of) the polarizability in different regions.

Within this region of anomalous absorption, the imaginary part grows without limit at $\varepsilon_r = +4, \varepsilon_t = -1/2$, and it vanishes for large absolute values of ε_r or ε_t. The real part of the polarizability is zero when

$$\varepsilon_t = -\frac{\varepsilon_r+4}{4\varepsilon_r}, \qquad -2 < \varepsilon_r < 4. \quad (16)$$

Approaching the point $\varepsilon_r = +4, \varepsilon_t = -1/2$ along the curve (16), we thus get a purely imaginary polarizability that grows without limit even if the intrinsic parameters ε_r and ε_t are real.

2.3. Plasmonic Resonances, Invisibility, Perfect Electric Conductor, and Perfect Magnetic Conductor

The anomalous absorption is, arguably, the most peculiar feature of the RA sphere, but we can

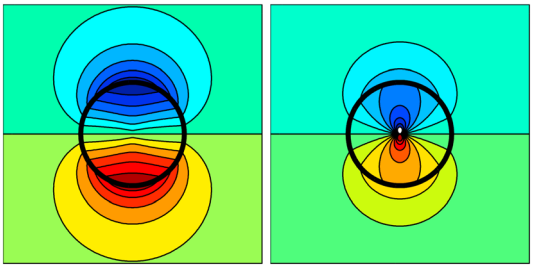

Figure 3. A cross cut of the total electrostatic potential distribution of an RA sphere in a uniform vertical static electric field. (left) $\varepsilon_r = -3$, $\varepsilon_t \approx -5/3$. The surface plasmon resonance yields singular polarizability. (right) $\varepsilon_r = 5$, $\varepsilon_t = -3/5$. In this hyperbolic case, the singular polarizability is due to the resonance that occurs in the core of the sphere.

also find a few other interesting special cases. As is easily seen from (14), the polarizability is infinite when $\varepsilon_{\text{eff}} = -2$ and zero when $\varepsilon_{\text{eff}} = 1$. Both of these extreme cases could be interesting for very different reasons.

The polarizability is singular, and $\varepsilon_{\text{eff}} = -2$, when

$$\varepsilon_t = \frac{2 - \varepsilon_r}{\varepsilon_r}, \qquad \varepsilon_r < 0,\ \varepsilon_r > 4. \tag{17}$$

These conditions are visualized in Figure 2. We can see that there are two types of singularities: in the third and fourth quadrants. The first one is a surface plasmon which is a generalization of the $\varepsilon = -2$ resonance of an isotropic sphere (see Figure 3 (left)). However, another type of singularity is found for certain combinations of $\varepsilon_t < 0$ and $\varepsilon_r > 0$ which correspond to a resonance that is located in the core of the RA sphere, visualized in Figure 3 (right). In both panels of Figure 3, the total potential solution given by (8) is plotted.

The latter kind of singularity is in a way a combination of two fundamentally different singularities: the potential is singular at the origin, since ν is real but negative, and the overall response (quasistatic polarizability) is also singular, since $\varepsilon_{\text{eff}} = -2$. Including losses will certainly dampen both the singularity at the origin and the infinite polarizability, and so it seems that this kind of singularity is perhaps not the best option if we need to design a strong polarizability using lossy material.

The RA sphere is invisible for a uniform static electric field when the polarizability vanishes. In the presently studied ideal case, this happens for $\varepsilon_{\text{eff}} = 1$ when

$$\varepsilon_t = \frac{\varepsilon_r + 1}{2\varepsilon_r}, \qquad \varepsilon_r < -2,\ \varepsilon_r > 0. \tag{18}$$

Again, there are two "types" of invisibility. Like an isotropic sphere is invisible for $\varepsilon = +1$, an increase of ε_r can be compensated by decreasing ε_t and vice versa in the first quadrant of Figure 2 to retain zero polarizability. As shown in *Kettunen et al.* [2013], the choice $0 < \varepsilon_r \ll 1, \varepsilon_t \gg 1$ also yields a design for a cloak (see Figure 4 (left), where the total potential is plotted as in Figure 3). However, the RA sphere can also be invisible even if ε_r is negative, according to (18) with $\varepsilon_r < -2$ (see Figure 4 (right)). This is a very peculiar situation because the potential is singular at the origin at the same time. Again, this configuration is certainly sensitive to losses, but it could perhaps even in the lossy case be possible to design an almost invisible RA sphere with large field concentration in the center.

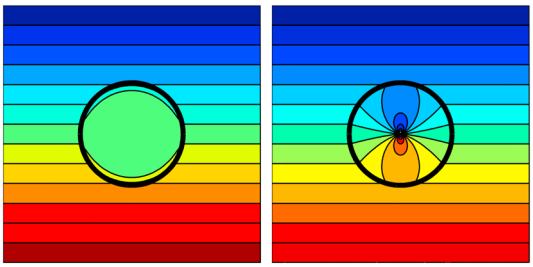

Figure 4. A cross cut of the total electrostatic potential distribution of an RA sphere in a uniform vertical static electric field. (left) $\varepsilon_r = 0.1$, $\varepsilon_t = 5.5$. The constant (zero) potential at the core becomes stretched and can be applied in cloaking smaller inclusions from the external field. (right) $\varepsilon_r = -3$, $\varepsilon_t = 1/3$. The sphere is invisible for an outside observer, even though the potential is singular at the origin.

In electrostatics, a perfect electric conductor (PEC) is characterized by $\varepsilon \to \infty$, and a perfect magnetic conductor (PMC) corresponds to $\varepsilon = 0$. As is easily seen from (14), the polarizability of a PEC sphere is +3 and the polarizability of a PMC sphere is $-3/2$. The RA sphere behaves like a PMC sphere if either ε_r or ε_t is zero. On the other hand, the RA sphere becomes identical to a PEC sphere ($\alpha = +3$) if $\varepsilon_t \to \pm\infty$. However, a large value of ε_r is not sufficient to make the RA sphere PEC like: the limit depends on ε_t

$$\lim_{\varepsilon_r \to \infty} \alpha = \frac{3}{2} \cdot \frac{2\varepsilon_t - 1}{\varepsilon_t + 1}. \tag{19}$$

2.4. Punctured RA Sphere

The troublesome point of the intact RA sphere is the origin, where the permittivity dyadic is

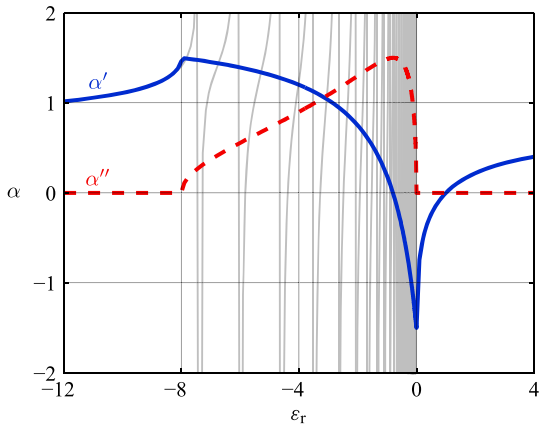

Figure 5. Normalized static polarizability $\alpha' - j\alpha''$ of the intact RA sphere (thick lines) compared with the punctured case with $b/a = 10^{-10}$ (thin gray line). The tangential permittivity is constant $\varepsilon_t = 1$.

also undefined. Due to the symmetry of the geometry and the excitation, the potential must be zero at the whole x-y plane as is also evident from the factor $\cos\theta$ in (7)–(10). In particular, the potential is zero at the origin, and so it seems reasonable to remove the origin by explicitly grounding it. More precisely, let us assume that there is a grounded PEC sphere of radius $b < a$ at the origin and study the limit $b/a \to 0$. In the punctured case, we thus seek the solution in the form

$$\phi(r,\theta) = \begin{cases} 0, & r \le b, \\ \phi_i(r,\theta), & b < r < a, \\ \phi_0(r,\theta) + \phi_s(r,\theta), & r > a, \end{cases} \tag{20}$$

where ϕ_0 and ϕ_s have the same form as for the intact sphere in (7) and (10). The internal potential is

$$\phi_i(r,\theta) = \left[A'\left(\frac{r}{a}\right)^{\nu} + B'\left(\frac{r}{a}\right)^{-\nu-1}\right]\cos\theta. \tag{21}$$

The constants A' and B' of (21) and B of (10) can be derived by enforcing the boundary condition $\phi_i(b,\theta) = 0$ and the interface conditions (11). After straightforward but somewhat lengthy algebraic manipulations, the polarizability takes the familiar form

$$\alpha = 3\frac{\varepsilon_{\text{eff}} - 1}{\varepsilon_{\text{eff}} + 2}, \tag{22}$$

with the effective permittivity

$$\varepsilon_{\text{eff}} = \frac{\varepsilon_r}{2}\left(-1 + \sqrt{\cdot}\,\frac{1 + \left(\frac{b}{a}\right)^{\sqrt{\cdot}}}{1 - \left(\frac{b}{a}\right)^{\sqrt{\cdot}}}\right), \tag{23}$$

where

$$\sqrt{\cdot} = \sqrt{1 + 8\varepsilon_t/\varepsilon_r} = 2\nu + 1. \tag{24}$$

The coefficients for the internal potential (21) are

$$A' = \frac{-3U_0}{(\varepsilon_{\text{eff}} + 2)\left(1 - \left(\frac{b}{a}\right)^{\sqrt{\cdot}}\right)}, \tag{25}$$

$$B' = -\left(\frac{b}{a}\right)^{\sqrt{\cdot}} A'. \tag{26}$$

This solution for the punctured RA sphere is real and finite for any $b > 0$ and real $\varepsilon_r, \varepsilon_t$. The imaginary parts cancel out exactly, although it is not immediately obvious from the above formulas.

If the square root (24) is real, i.e., $\varepsilon_t/\varepsilon_r > -1/8$, the limit

$$\lim_{b\to 0}\left(\frac{b}{a}\right)^{\sqrt{\cdot}} = 0 \tag{27}$$

is well defined and we get the intact RA solution when the PEC core vanishes. If $\varepsilon_t/\varepsilon_r < -1/8$, the square root (24) is purely imaginary and the limit does not exist since

$$\left(\frac{b}{a}\right)^{\pm j\beta} = \cos\left(\beta \ln\frac{b}{a}\right) \pm j\sin\left(\beta \ln\frac{b}{a}\right), \tag{28}$$

which oscillates without reaching a limit when $b/a \to 0$.

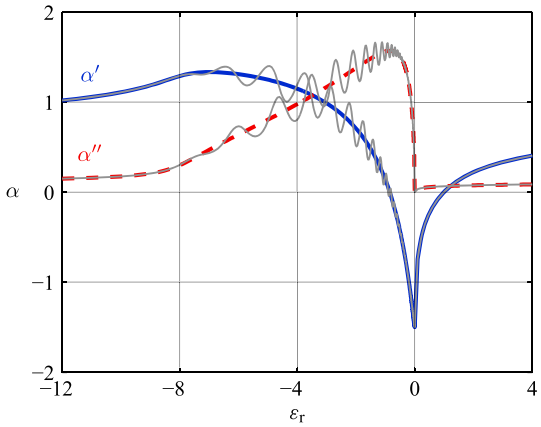

Figure 6. Normalized static polarizability, as in Figure 5, with added losses in the tangential permittivity $\varepsilon_t = 1 - j/10$. There is clearly a much better agreement between the intact and punctured cases.

Hence, in the lossless case, when $\varepsilon_t/\varepsilon_r < -1/8$, we fail to achieve consistency between the solutions for the intact sphere and the punctured sphere with vanishing core radius. While the former yields a complex polarizability (effective losses), the latter solution does not converge. Figure 5 shows a comparison between the two solutions for a particular choice of very small but nonzero b/a. Neither solution seems reasonable, but the ambiguity is very similar to the branch cut or unlimited number of singularities that arise in geometries containing sharp corners and certain ranges of negative permittivity [*Kettunen et al.*, 2008; *Wallén et al.*, 2008; *Pitkonen*, 2010; *Helsing et al.*, 2011; *Alù and Engheta*, 2011; *Mohammadi Estakhri and Alù*, 2013]. Although the geometry is very different, both the sharp corner and the RA sphere admit a similar kind of singularity for certain permittivity values. In both cases, the potential solution can be expressed in the form r^ν with a complex exponent ν, where r is the distance from either the sharp edge or the origin.

2.5. Punctured RA Sphere With Losses

The inconsistency between the two solutions can be relaxed by adding losses into the material. This makes the limit $b/a \to 0$ well defined. Using the time convention $e^{+j\omega t}$, small losses as a negative imaginary part of either ε_r and ε_t (or both) ensure that the real part of the square root (24) is nonzero, which is sufficient to make the limit (27) vanish. Therefore, the solution for the punctured RA sphere approaches the one for the intact RA sphere, as long as there are some material losses involved. This argument is valid for arbitrarily small intrinsic losses, and thus, it gives credibility to the earlier result of complex RA polarizability for $\varepsilon_t/\varepsilon_r < -1/8$, and the associated anomalous losses. However, the result for real permittivity components must be understood as an approximation where the losses are infinitesimally small.

Figure 6 shows the polarizability of a punctured sphere with modest losses and very small b/a. The polarizability of the punctured sphere agrees fairly well with the polarizability calculated from the result of the intact RA sphere.

The result for the punctured lossy sphere is remarkably different from the lossless case shown in Figure 5 in the hyperbolic region where the intact sphere exhibits anomalous absorption. We can thus, both analytically and numerically, conclude that the solution for the lossless punctured RA sphere in section 2.4 is meaningful only for nonvanishing core radius. The (infinitesimally small) intrinsic losses in the material parameters are essential to get a physically meaningful result, for all ε_t and ε_r, for the intact sphere as the limit of a punctured sphere with vanishing core radius.

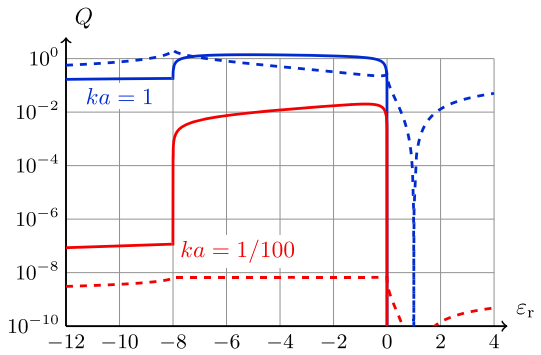

Figure 7. Absorption efficiency Q_{abs} (solid lines) and scattering efficiency Q_{sca} (dashed lines) for an RA sphere with two different size parameters $x = ka$. In both cases $\varepsilon_t = 1$. Especially for the electrically small RA sphere, the absorption due to the electric dipole term a_1 dominates in the region $-8 < \varepsilon_r/\varepsilon_t < 0$, as predicted by the quasistatics.

3. Mie Scattering for an RA Sphere

The scattering of a plane wave from an RA sphere of arbitrary size can be solved using a slight modification of the classical Mie series solution. Compared with the formulas in chapter 4 of *Bohren and Huffman* [1983], the main modification is that the degrees of the spherical Bessel functions in the sphere are $\nu(n)$ given by (6) instead of n. (Also notice the trivial difference

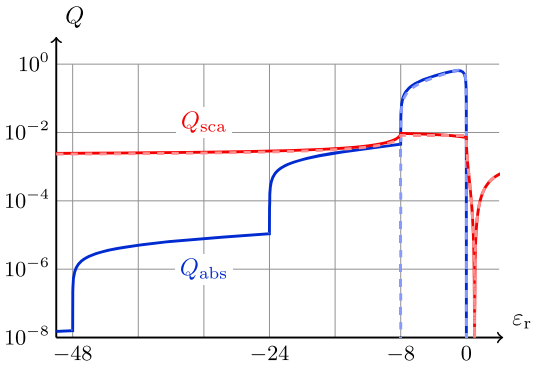

Figure 8. Absorption and scattering efficiencies (solid lines) compared with the quasistatic approximation (dashed lines) for an RA sphere with size parameter $x = ka = 1/3$. The transversal permittivity is $\varepsilon_t = 1$, as in Figure 7.

in time convention.) As in the static case, we can interpret the radial anisotropy as a stretching of the r coordinate inside the sphere.

In agreement with *Luk'yanchuk and Qiu* [2008] and *Qiu et al.* [2010], we get the scattering coefficients

$$a_n = \frac{m\psi_\nu(mx)\psi_n'(x) - \psi_n(x)\psi_\nu'(mx)}{m\psi_\nu(mx)\xi_n'(x) - \xi_n(x)\psi_\nu'(mx)}, \tag{29}$$

and

$$b_n = \frac{\psi_n(mx)\psi_n'(x) - m\psi_n(x)\psi_n'(mx)}{\psi_n(mx)\xi_n'(x) - m\xi_n(x)\psi_n'(mx)}, \tag{30}$$

where $m = \sqrt{\varepsilon_t}$ is the tangential refractive index and $x = ka$ is the size parameter. The Riccati-Bessel functions are defined in terms of ordinary spherical Bessel functions as $\psi_\nu(x) = xj_\nu(x)$ and $\xi_\nu(x) = xh_\nu^{(2)}(x)$. To get an overall measure of the response of the sphere, we study the scattering, extinction, and absorption efficiencies

$$Q_{sca} = \frac{2}{x^2}\sum_{n=1}^{\infty}(2n+1)\left(|a_n|^2 + |b_n|^2\right), \tag{31}$$

$$Q_{ext} = \frac{2}{x^2}\sum_{n=1}^{\infty}(2n+1)\,\mathrm{Re}\{a_n + b_n\}, \tag{32}$$

$$Q_{abs} = Q_{ext} - Q_{sca}. \tag{33}$$

In the dynamic treatment, Q_{abs} gives a measure for the losses of the scatterer. The absorption efficiency should be zero for lossless (real) material parameters. Indeed, this is the case for RA spheres with $\varepsilon_r/\varepsilon_t > 0$.

However, like in the static analysis, we notice anomalous absorption for hyperbolic radial anisotropy. This can be seen in Figure 7 which shows the absorption efficiencies of electrically small and moderate RA spheres for which the tangential permittivity is unity, but the radial component varies over a wide negative range. The absorption is related to the electrical multipole of degree n with coefficients a_n. The degree $\nu(n)$ of (6) is complex when $-4n(n+1) < \varepsilon_r/\varepsilon_t < 0$, and this gives rise to effective losses in the corresponding electric multipole. The most significant absorption is given by the electrical dipole term a_1, exactly as predicted by the quasistatic approximation, but also, the higher-order multipoles contribute to the losses. Notice how the limits $\varepsilon_r/\varepsilon_t = -8$ ($n = 1$), $\varepsilon_r/\varepsilon_t = -24$ ($n = 2$), and $\varepsilon_r/\varepsilon_t = -48$ ($n = 3$) stand out in Figure 8, which shows the absorption and scattering efficiencies for an RA sphere of modest size compared with the quasistatic approximation.

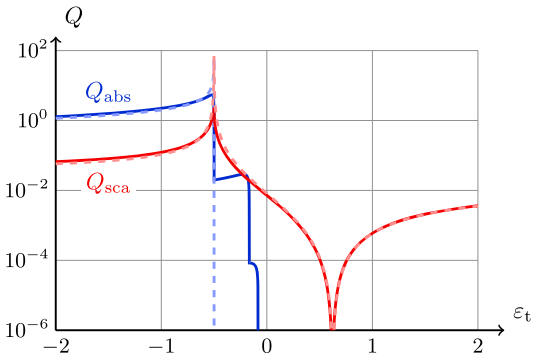

Figure 9. Absorption and scattering efficiencies (solid lines) compared with the quasistatic approximation (dashed lines) for an RA sphere with size parameter $x = ka = 1/3$. The radial permittivity is $\varepsilon_r = 4$.

The scattering efficiency of a small hyperbolic RA sphere is typically small compared with the absorption as shown also in Figures 7 and 8. Small RA spheres can also exhibit strong scattering, in a similar way as small isotropic spheres with negative permittivity. As shown in *Luk'yanchuk and Qiu* [2008] and *Qiu et al.* [2010], these resonances can be shifted by adjusting ε_r

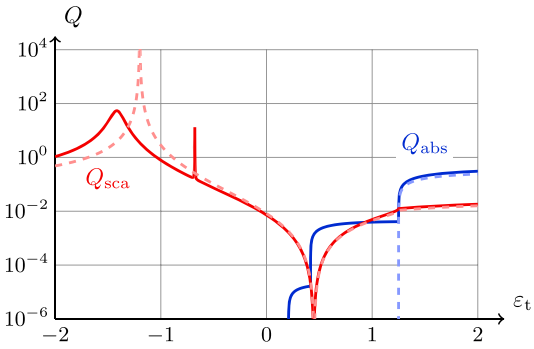

Figure 10. Absorption and scattering efficiencies (solid lines) compared with the quasistatic approximation (dashed lines) for an RA sphere with size parameter $x = ka = 1/3$. The radial permittivity is $\varepsilon_{\mathrm{r}} = -10$.

and ε_{t}, but the strongest scattering appears to always be found when both ε_{r} and ε_{t} are negative. This is clearly different from the anomalous absorption, which can only be found when ε_{r} and ε_{t} are of opposite signs. In Figures 9 and 10, the scattering and absorption efficiencies are plotted for varying tangential permittivity component with fixed radial component. The resonant scattering stands out for the case of both permittivity components being negative (Figure 10) as compared to the hyperbolic case (Figure 9) where the scattering singularity is shadowed by the extreme absorption.

In the small parameter limit ($x = ka \ll 1$), we can write the asymptotics for the generalized Mie coefficients (29) and (30). The dominant coefficient is

$$a_1 = j\frac{2}{9}\alpha x^3 + \mathcal{O}(x^5), \tag{34}$$

and the rest of the coefficients are $\mathcal{O}(x^5)$ or smaller. Keeping only the term a_1 gives the quasistatic approximations for the efficiencies

$$Q_{\mathrm{sca}} \approx \frac{8}{27}|\alpha|^2 x^4 \tag{35}$$

and

$$Q_{\mathrm{abs}} \approx \frac{4}{3}\alpha'' x, \tag{36}$$

where $\alpha = \alpha' - j\alpha''$ is the static normalized polarizability. It is worth noting that even if these approximations are derived for a small RA sphere, they agree with the small parameter limit for the isotropic sphere [*Bohren and Huffman*, 1983, chap 5]. That is, the radial anisotropy can have a dramatic effect on the polarizability, but the expressions (35) and (36) are formally the same as for an isotropic sphere.

This small parameter approximation is valid for all ε_{r} and ε_{t} except for the special case (17) corresponding to $\varepsilon_{\mathrm{eff}} = -2$. This special case is, however, only possible in the perfectly lossless case, and we can thus ignore it by assuming at least some infinitesimally small losses in the material.

Figures 8–10 make the comparison between the full dynamic, (31) and (33), and quasistatic, (35) and (36), absorption and scattering efficiencies for spheres with size parameter $x = 1/3$. We can observe that the dipolar term of the absorption efficiency Q_{abs} is surprisingly accurately predicted by the quasistatic approximation, but the much weaker higher-order terms are omitted in the quasistatics. Moreover, the quasistatic scattering efficiency Q_{sca} agrees very well with the dynamic one, except near the surface plasmon resonance where both ε_{r} and ε_{t} are negative (see Figure 10). The quasistatic approximation only gives one resonant peak in the scattering efficiency Q_{sca} when $\varepsilon_{\mathrm{eff}} = -2$. The dynamic solution also excites resonances of higher order, and these higher-order resonances play a larger role as the size parameter increases. Hence, it is quite expected that the largest discrepancy between the quasistatic and dynamic solutions can be observed near the surface plasmon resonances. For smaller size parameters, the agreement improves. Anomalous absorption, resonant singularities, and invisibility properties of small spheres can thus be qualitatively and quantitatively analyzed using the quasistatic results.

4. Conclusions

A radially anisotropic (RA) sphere responds to electromagnetic excitation in a nontrivial way. The present paper analyzed this interaction both for electrostatic and full electrodynamic excitation, where the comparison between the quasistatic and dynamic scattering and absorption responses of the RA sphere showed that the quasistatic polarizability agrees surprisingly well with the dynamic result even up to electrical size

$ka = 1/3$ of the sphere. In particular, the focus was on the peculiarities of indefinite or hyperbolic RA spheres, for which the tangential and radial permittivity components have different signs.

It was shown that if the ratio between the tangential and radial permittivities is less (more negative) than $-1/8$, the quasistatic polarizability is a complex number, even if the intrinsic permittivity components are real. A careful limiting treatment with a punctured, weakly lossy RA sphere showed the consistency of the result for the intact RA sphere. In particular, the puncturing was needed to remove the singularity of the potential at the origin and nonzero losses are essential to get a well-defined limit for vanishing core radius. The anomalous absorption was also found in the dynamic response of the hyperbolic RA sphere. The absorption enhancement property of RA spheres naturally gives an idea of realizing effective absorbing materials as composites made of hyperbolic RA spheres. On the other hand, RA spheres made of active materials [*Hess et al.*, 2012] could realize effective signal amplifying gain materials. Mathematically, this means just changing the signs of the imaginary parts in the current analysis.

The RA sphere can also display two types of singularities: a generalized surface plasmon resonance when both the tangential and radial permittivities are negative, and also a weaker type of resonant singularity in the hyperbolic regime.

The invisibility properties of RA spheres were also considered, and two types of anisotropies producing zero polarizability were found. A combination of positive and nonequal permittivity components can be found to make the RA sphere vanish in electric excitation. In particular, if the tangential permittivity component is large (and consequently, the radial is a positive number less than one), the sphere can be used as a cloaking structure: in the long-wavelength limit, the interior of the sphere is very effectively shielded from the external field, and hence, the core of the sphere can be removed and the cavity acts as a Faraday cage. This cloaking approach could thus be a promising alternative to the plasmonic cloaking approach by *Alù and Engheta* [2008]. Both approaches are essentially quasistatic. The plasmonic cloaking approach is arguably easier to implement, while the RA cloak is less dependent on the object that is to be cloaked.

However, there is also another type of invisibility: the polarizability of the RA sphere can vanish in the hyperbolic regime. In this case the potential displays a singularity in the origin.

The capability of an RA sphere to strongly focus the electric field (and energy) into its origin seems very beneficial considering applications in sensing and energy harvesting. Figure 4 (right) presented an RA sphere that has a strong focusing effect in the origin without disturbing the external field. This configuration clearly offers a possibility of constructing an invisible sensor. Moreover, replacing the core of such sphere with a nonlinear material gives an opportunity to realize devices tunable by the amplitude of the external field. This could lead way to optical switches and memories.

Since the current study has been based on quite idealized material parameters, further research should consider how (hyperbolic) RA spheres could actually be realized. We could also study the broadband behavior of RA spheres using realistic material models (e.g., Drude or Lorentz) including the effects of losses and frequency dispersion. It is certainly interesting to see how, for example, the focusing and cloaking performances are affected by losses, and how broadband these properties are when material parameters are changing due to dispersion. On the other hand, we might want to tune the desired response to be extremely narrow band to design RA devices for filtering purposes.

Acknowledgments
The work of H. Kettunen was supported by the Academy of Finland projects 260522 and CoE-250215. All data used in the figures have been generated using the formulas in the paper. Please contact the corresponding author if you need the plotted data in numerical format.

References

Alù, A., and N. Engheta (2008), Robustness in design and background variations in metamaterial/plasmonic cloaking, *Radio Sci.*, *43*, RS4S01, doi:10.1029/2007RS003815.

Alù, A., and N. Engheta (2011), Extremely anisotropic boundary conditions and their optical applications, *Radio Sci.*, *46*, RS0E11, doi:10.1029/2011RS004679.

Bohren, C. F., and D. R. Huffman (1983), Absorption and scattering of light by small particles.

Chettiar, U. K., and N. Engheta (2012), Internal homogenization: Effective permittivity of a coated sphere, *Opt. Express*, *20*(21), 22,976–22,986, doi:10.1364/OE.20.022976.

de Munck, J. C. (1988), The potential distribution in a layered anisotropic spheroidal volume conductor, *J. Appl. Phys.*, *64*(2), 464–470, doi:10.1063/1.341983.

Gao, L., T. H. Fung, K. W. Yu, and C. W. Qiu (2008), Electromagnetic transparency by coated spheres with radial anisotropy, *Phys. Rev. E.*, *78*(4), 046609, doi:10.1103/PhysRevE.78.046609.

Geng, Y., X. Wu, and L.-W. Li (2003), Analysis of electromagnetic scattering by a plasma anisotropic sphere, *Radio Sci.*, *38*(6), 1104, doi:10.1029/2003RS002913.

Geng, Y.-L., X.-B. Wu, L.-W. Li, and B.-R. Guan (2004), Mie scattering by a uniaxial anisotropic sphere, *Phys. Rev. E*, *70*, 56609, doi:10.1103/PhysRevE.70.056609.

Helsing, J., and A. Helte (1991), Effective conductivity of aggregates of anisotropic grains, *J. Appl. Phys.*, *69*(6), 3583–3588, doi:10.1063/1.348501.
Helsing, J., R. C. McPhedran, and G. W. Milton (2011), Spectral super-resolution in metamaterial composites, *New J. Phys.*, *13*(11), 115005, doi:10.1088/1367-2630/13/11/115005.
Hess, O., J. B. Pendry, S. A. Maier, R. F. Oulton, J. M. Hamm, and K. L. Tsakmakidis (2012), Active nanoplasmonic metamaterials, *Nat. Mater.*, *11*(7), 573–584, doi:10.1038/nmat3356.
Johnson, P. B., and R. W. Christy (1972), Optical constants of the noble metals, *Phys. Rev. B*, *6*(12), 4370–4379, doi:10.1103/PhysRevB.6.4370.
Karacali, H., S. M. Risser, and K. F. Ferris (1997), Scattering of light from small nematic spheres with radial anisotropy, *Phys. Rev. E*, *56*(4), 4286–4293, doi:10.1103/PhysRevE.56.4286.
Kettunen, H., H. Wallén, and A. Sihvola (2008), Electrostatic resonances of a negative-permittivity hemisphere, *J. Appl. Phys.*, *103*(9), 094112, doi:10.1063/1.2917402.
Kettunen, H., H. Wallén, and A. Sihvola (2013), Cloaking and magnifying using radial anisotropy, *J. Appl. Phys.*, *114*(4), 044110, doi:10.1063/1.4816797.
Kiselev, A. D., V. Y. Reshetnyak, and T. J. Sluckin (2002), Light scattering by optically anisotropic scatterers: T-matrix theory for radial and uniform anisotropies, *Phys. Rev. E*, *65*(5), 056609, doi:10.1103/PhysRevE.65.056609.
Luk'yanchuk, B. S., and C.-W. Qiu (2008), Enhanced scattering efficiencies in spherical particles with weakly dissipating anisotropic materials, *Appl. Phys. A*, *92*(4), 773–776, doi:10.1007/s00339-008-4572-5.
Mei, Z., T. K. Sarkar, and M. Salazar-Palma (2013), A study of negative permittivity and permeability for small sphere, *IEEE Antennas Wirel. Propag. Lett.*, *12*, 1228–1231, doi:10.1109/LAWP.2013.2282331.
Mohammadi Estakhri, N., and A. Alù (2013), Physics of unbounded, broadband absorption/gain efficiency in plasmonic nanoparticles, *Phys. Rev. B*, 205418, doi:10.1103/PhysRevB.87.205418, (to appear in print).
Monzon, J. C. (1989), Three-Dimensional field expansion in the most general rotationally anisotropic material: Application to scattering by a sphere, *IEEE Trans. Antennas Propag.*, *37*(6), 728–735, doi:10.1109/8.29359.
Noginov, M., M. Lapine, V. Podolskiy, and Y. Kivshar (2013), Focus issue: Hyperbolic metamaterials, *Opt. Express*, *21*(12), 14,895–14,897, doi:10.1364/OE.21.014895.
Pitkonen, M. (2010), A closed-form solution for the polarizability of a dielectric double half-cylinder, *J. Electromagn. Waves Appl.*, *24*(8–9), 1267–1277, doi:10.1163/156939310791586106.
Poddubny, A., I. Iorsh, P. Belov, and Y. Kivshar (2013), Hyperbolic metamaterials, *Nat. Photonics*, *7*(12), 958–967, doi:10.1038/nphoton.2013.243.
Qiu, C., L. Gao, J. D. Joannopoulos, and M. Soljačić (2010), Light scattering from anisotropic particles: Propagation, localization, and nonlinearity, *Laser Photonics Rev.*, *4*(2), 268–282, doi:10.1002/lpor.200810078.
Qiu, C.-W., and B. Luk'yanchuk (2008), Peculiarities in light scattering by spherical particles with spherical anisotropy, *J. Opt. Soc. Am.*, *25*(7), 1623–1628, doi:10.1364/JOSAA.25.001623.
Qiu, C.-W., L.-W. Li, T.-S. Yeo, and S. Zouhdi (2007), Scattering by rotationally symmetric anisotropic spheres: Potential formulation and parametric studies, *Phys. Rev. E*, *75*(2), 026609, doi:10.1103/PhysRevE.75.026609.
Qiu, C.-W., A. Novitsky, H. Ma, and S. Qu (2009), Electromagnetic interaction of arbitrary radial-dependent anisotropic spheres and improved invisibility for nonlinear-transformation-based cloaks, *Phys. Rev. E*, *80*(1), 016604, doi:10.1103/PhysRevE.80.016604.
Rimpiläinen, T., H. Wallén, H. Kettunen, and A. Sihvola (2012), Electrical response of systropic sphere, *IEEE Trans. Antennas Propag.*, *60*(11), 5348–5355, doi:10.1109/TAP.2012.2207677.
Roth, J., and M. J. Dignam (1973), Scattering and extinction sections for a spherical particle coated with an oriented molecular layer, *J. Opt. Soc. Am.*, *63*(3), 308–311, doi:10.1364/JOSA.63.000308.
Schulgasser, K. (1983), Sphere assemblage model for polycrystals and symmetric materials, *J. Appl. Phys.*, *54*(3), 1380–1382, doi:10.1063/1.332161.
Smith, D. R., and D. Schurig (2003), Electromagnetic wave propagation in media with indefinite permittivity and permeability tensors, *Phys. Rev. Lett.*, *90*, 077405, doi:10.1103/PhysRevLett.90.077405.
Sten, J. C.-E. (1995), DC fields and analytical image solutions for a radially anisotropic spherical conductor, *IEEE Trans. Dielectr. Electr. Insul.*, *2*(3), 360–367, doi:10.1109/94.395424.
Wallén, H., H. Kettunen, and A. Sihvola (2008), Surface modes of negative-parameter interfaces and the importance of rounding sharp corners, *Metamaterials*, *2*(2–3), 113–121, doi:10.1016/j.metmat.2008.07.005.
Wallén, H., H. Kettunen, and A. Sihvola (2013), Singularities or emergent losses in radially uniaxial spheres, paper presented at 2013 International Symposium on Electromagnetic Theory (EMTS 2013) May 21-24, 2013 Hiroshima, Japan, pp. 388–390.
Wong, K.-L., and H.-T. Chen (1992), Electromagnetic scattering by a uniaxially anisotropic sphere, *IEE Proc. Parts H*, *139*(4), 314–318, doi:10.1049/ip-h-2.1992.0056.
Žumer, S. (1988), Light scattering from nematic droplets: Anomalous-diffraction approach, *Phys. Rev. A*, *37*(10), 4006–4015, doi:10.1103/PhysRevA.37.4006.
Žumer, S., and J. W. Doane (1986), Light scattering from a small nematic droplet, *Phys. Rev. A*, *34*(4), 3373–3386, doi:10.1103/PhysRevA.34.3373.